Nonlinear Dyn (2019) 98:2989–2999
https://doi.org/10.1007/s11071-019-05077-4

ORIGINAL PAPER

Control of imperfect dynamical systems

Maide Bucolo · Arturo Buscarino · Carlo Famoso · Luigi Fortuna · Mattia Frasca

Received: 21 December 2018 / Accepted: 15 June 2019 / Published online: 26 June 2019

Abstract Imperfections are unavoidable in production processes of real devices. Despite this, and despite the fact that real devices usually operate in regimes far from ideality, they still work. This is related to the fact that imperfections give rise to hidden dynamics, which, opportunely excited, have an overall positive effect on the device. In this paper, we focus on a complex and imperfect electromechanical structure which can be considered as a paradigm for imperfect systems. The electrical and mechanical interactions within the structure generate complex patterns of vibration which may prevent the system to reach the correct working conditions. A control strategy to ensure the optimal working conditions based on the excitation of the hidden dynamics induced by imperfections is discussed, characterizing its effect with respect to the control signal properties and to the power provided to the structure.

Keywords Imperfect systems · Vibrational control · Nonlinear circuits · Electromechanical systems

M. Bucolo · A. Buscarino (✉) · C. Famoso · L. Fortuna · M. Frasca
DIEEI, University of Catania, Catania, Italy
e-mail: arturo.buscarino@unict.it

A. Buscarino · L. Fortuna · M. Frasca
CNR-IASI, Italian National Research Council, Institute for Systems Analysis and Computer Science "A. Ruberti", Rome, Italy

1 Introduction

The class of imperfect dynamical systems has been only recently formally introduced [1,2]. Imperfection is ubiquitous in engineered devices: It may be originated by the properties of the materials involved in the construction processes or even by the processes themselves [3]. The classical approach toward imperfection consists in considering it as a source of uncertainty, either structural or parametric. Therefore, production processes are oriented toward modeling and minimizing the effects of uncertainty. Even from a control perspective, uncertainty is explicitly taken into consideration by defining suitable control strategies which are robust and insensitive with respect to imperfections.

Analogously to the well-known positive effect that a suitable level of noise can have [4], it has been observed that imperfection itself is beneficial and exploiting it is possible to improve the working conditions of the system on which it acts. There are numerous examples of systems and devices whose characteristic behavior would not exist in ideal conditions: A imperfect wheel rotates over a surface thanks to friction [1], some analog circuits are able to show complex oscillations, including chaos, only thanks to parasitic effects at the nanoscales [5], even in controlling robots locomotion, erratic control signals may improve the motion capabilities [6].

In this paper, we will describe the behavior and the control perspective of the class of dynamical systems

named *imperfect uncertain systems*. Due to their intrinsically imperfect structure, for this class of systems, usual control techniques may fail. On the contrary, the idea of our paper is to use only few actions in order to control the whole system by eliciting its intrinsic properties of self-organization as an effect of the stimulation of the imperfect dynamics by means of broadband chaotic signals. Therefore, the control system will consist of an on/off controller generating the broadband spectrum signal and stimulating the hidden dynamics of the system.

As a paradigmatic example of imperfect uncertain systems, we will refer to a large-scale electromechanical system characterized by intermittent unmodeled dynamics and uncertain parameters. Such system consists of a high order vibrating round structure on which a series of coils rotating through the interaction of magnetic devices are allocated and allows for assess the experimental suitability of the proposed control strategy.

Indeed the control of imperfect systems is particularly appealing when we consider a large number of units, making the system with an high number of state variables. The control strategy proposed in this paper can be considered as a vibrational control [7] acting on the hidden dynamics related to imperfections. Moreover, the positive effect which can be observed by inducing external vibrations to a vibrating structure resembles what observed in vibrational resonance [8], a phenomenon consisting in the amplification of a weak low-frequency character signal. Instead of using high-frequency [9] or stick–slip vibrating [10] auxiliary signals, we exploit the broadband irregular nature of deterministic chaos.

The paper is organized as follows: In Sect. 2, the electromechanical structure and the control action are described; in Sect. 3, the control strategy and the hardware needed to generate the control signals are discussed; Sect. 4 discusses the experimental results and Sect. 5 draws the conclusions of the paper.

2 The electromechanical round system

The electromechanical system considered in this paper is based on a low weight mechanical structure [11] which acts at the same time as a support and as a power supply for the simple coils allocated over it. The overall system is reported in Fig. 1. Coils are realized winding a copper wire so that forms a diameter of 20 mm ring, as the one reported in Fig. 2a. To each coil is associated a neodymium magnet (N45) which is located over a passive support, not attached to the structure, below each coil slot at a distance of about 1 cm. While the supporting structure provides the current flowing through the coils, the magnets provide a magnetic field of intensity $B \approx 0.03$ T [12], whose interaction with the electrical field allows the coil rotation. A schematic representation of the single rotating coil, along with the geometric parameter values and the associated magnet, is reported in Fig. 2b.

The coils are manually realized in our laboratory, so that they must be considered as nonlinear imperfect systems, due to the practical difficulties in realizing

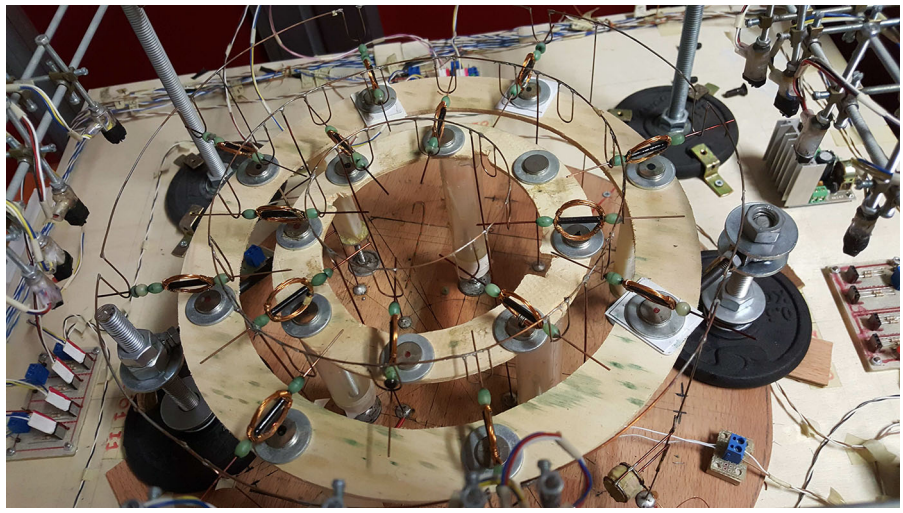

Fig. 1 View of the electromechanical structure and of the complete setup

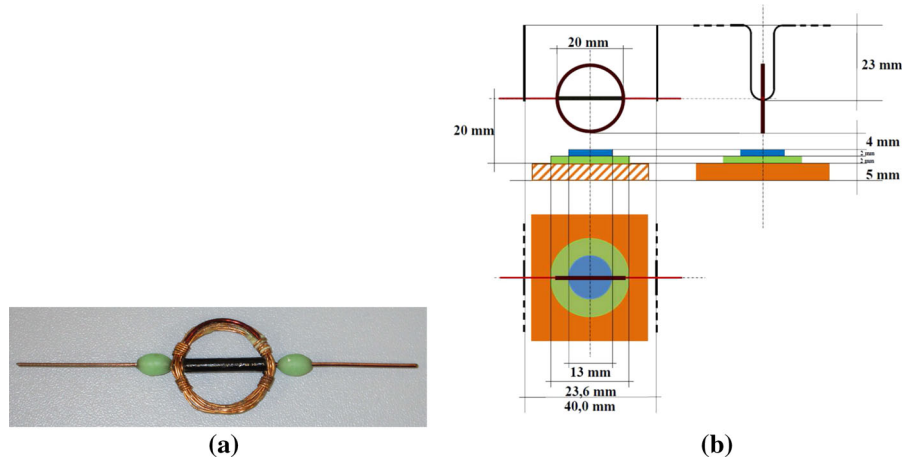

Fig. 2 **a** Picture of a single coil; **b** schematic representation of the coil-magnet system: the neodymium magnet is represented in blue, the magnet support in green and the plastic beam in orange. (Colour figure online)

identical coils. Each coil is realized by 10 windings of a copper wire with a cross section of 0.5 mm. The wire is covered by a layer of phenolic resin creating an insulating coating which has been preserved on a side of the surface, while was completely removed, exposing the copper conductive part, on the other side. This process is fundamental to obtain a permanent rotation of the coil along its axis, since if the coating is removed completely, the coil would short-circuit the power supply.

The support-power system is made by two wires with section of 1 mm and has been designed so that the interaction of the coil with the magnetic field is maximized.

The realization process of each part of the electromechanical structure introduces imperfections which affect the construction parameters, i.e., size and weight of the coils, balance of the supporting trails, but also the electromechanical interaction between coils, magnets and the supporting structure which provides power.

When the coil is oriented in the direction orthogonal to the magnet, it can be either or not in conduction. In conduction, the current, flowing through the coil, generates a field which produces a torque able to induce the coil motion along the horizontal axis. During the rotation, the conductive area alternates with the insulated area determining the interruption of the current. Thanks to the inertia, the coil is able to overcome the friction continuing its rotatory motion. As long as the support of the coil is powered, the alternating on/off cycle repeats producing a continuous rotation of the coil.

The coil motion inside the slots where they are located, in fact, is due to the geometrical imperfections of the electromechanical structure, and it is the reason for which horizontal and vertical vibrations arise in the structure.

The choice of the system that allows to measure the angular speed of coils is fundamental [2]. The tachometric system must be reliable, providing a measurement as accurate as possible, and, at the same time, not affecting the rotatory motion of the coil and its dynamics. In the choice of the measuring system, mechanical or magnetic sensors have been excluded, since their adoption would introduce a significant interaction with the dynamical behavior of the coils. The choice has settled on a reflection optical system capable of retrieving the passage of a reference element located on the coil itself. In such a system, in order to avoid that the ambient light influences the measurement, we have chosen a light source with a wavelength far from the visible range. In choosing the suitable sensor, the cost of the equipment has been also taken into account.

In order to fulfill all the requirements, we selected a reflective optical sensor with transistor output, namely the TCRT5000 produced by Vishay Semiconductors [13]. This device is very compact in size ($L \times W \times H$ in mm: $10.2 \times 5.8 \times 7$), robust in operation and, in the same package, contains the infrared photodiode emitter and the phototransistor detector. The latter is provided with filter block for the ambient light in the visible.

In order to actuate the structure with the designed control law, the control signal, which is a voltage, must be converted in a mechanical displacement. Therefore, the mechanical structures have been modified adding suitably located actuators [14].

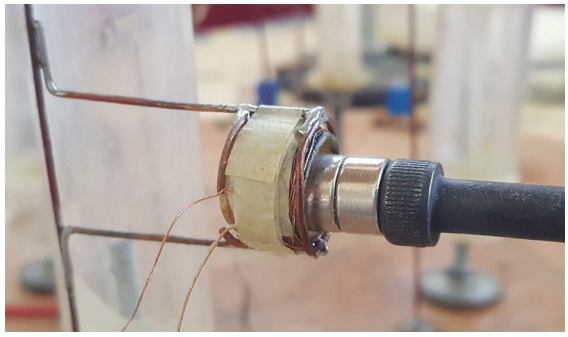

Fig. 3 Detail of the actuation system: configuration of the solenoid–magnet system

The actuation system is based on a solenoid located in points peculiar of the specific structure. The solenoid is powered by a current and interact with a permanent magnet constituting an electromagnetic actuator. It is built by 110 windings over a cylindrical support with diameter of 1 cm, using 7 m of isolated copper string (0.14 mm diameter, 0.015 mm^2 area of the section) providing a resistance of 8 Ω. Using a solenoid allows to control the magnetic force either in voltage or in current. Moreover, the actuation system has a short response time and a low impedance. The field associated with the solenoid is parallel to its axis and uniform. Its intensity and direction are proportional to the magnitude and direction of the current flowing in the windings.

The permanent magnet coupled with the solenoid is a sintered Neodymium (NdFeB) magnet with a nickel plating (Ni–Cu–Ni) of the class N45 providing a magnetic force of 2.5 kg. The magnet is located on a fixed support in order to maintain its relative position with respect to the solenoid. As shown in Fig. 3, the magnet is located within the solenoid, ensuring to the solenoid the possibility to move and produce a displacement orthogonal to the piers supporting the structure.

The interplay between the magnet and the solenoid depends on the current, therefore a mutual repulsive action is generated by opposite magnetic fluxes; otherwise, a mutual attractive action is due to parallel magnetic fluxes. The vibration is induced on the structure alternating the direction of the current through the solenoid according to the polarity of the vibrational control signal. The power is supplied to the solenoids through an amplifier based on the TDA7297 [15,16]. The circuit, whose schematic is reported in Fig. 4, is a two-channel audio amplifier able to provide to an impedance of 8 Ω a power up to 15 W per channel. We chose to adopt this scheme, whose implementation is reported in Fig. 5, since it is easy, reliable and low cost. The gain of the amplifier can be set acting on a single potentiometer.

The location of the actuation system with respect to the structure plays a crucial role on the effective provided momentum. From tests carried out, we have found that the presence of the actuators on the piers of the inner circumference is not effective for the entire structure, due to the higher stiffness of inner part of the structure, and only the coils of the inner ring feel the effect. Conversely, positioning the actuators on the piers of the outer ring leads to an opposite behavior: The higher flexibility of the structure lets the solicita-

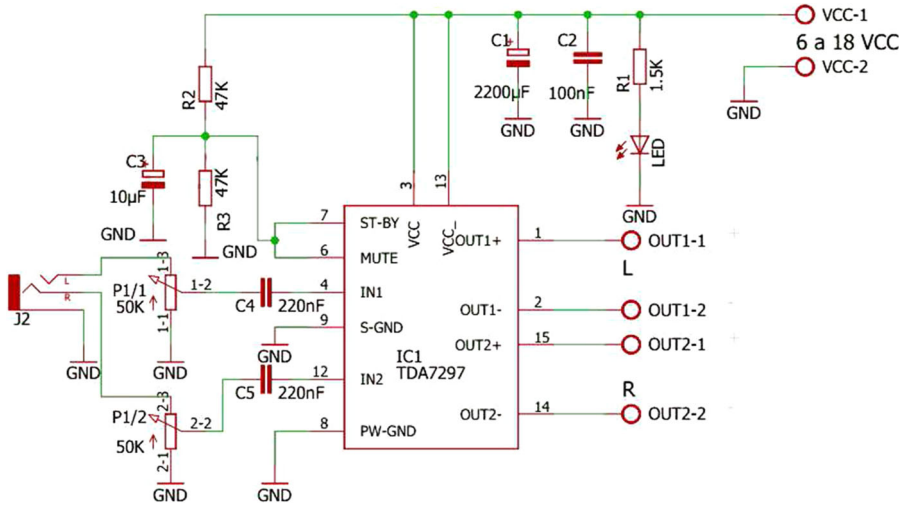

Fig. 4 Schematic of the amplifier driving the actuation system

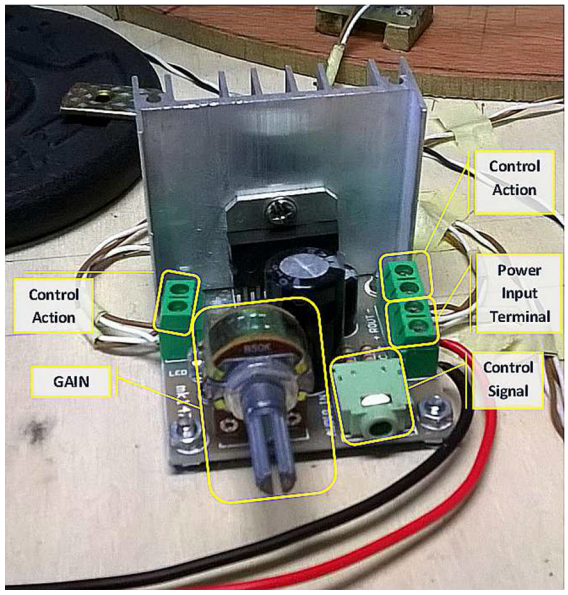

Fig. 5 Circuit implementation of the amplifier driving the actuation system

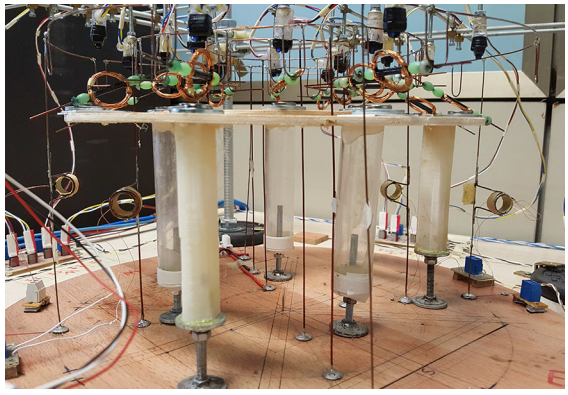

Fig. 6 Location of the two anti-phase actuators for the round structure

tion to be absorbed without transmitting it to the inner and central parts. The two actuators are located in correspondence to two diametrically opposed piers supporting the middle ring, as reported in Fig. 6. In this case, the two actuators may work in-phase or in anti-phase.

3 Mathematical model and design of the control law

From a mathematical point of view, an imperfect uncertain system can be described by a set of interacting state-space equations, some of which modeling the imperfect dynamics. In particular, we consider continuous-time models, so that the equations can be written as:

$$\begin{aligned} \dot{x} &= f(x, \tilde{x}, u, w, p, t) \\ \dot{\tilde{x}} &= \tilde{f}(x, \tilde{x}, u, w, p, t) \end{aligned} \tag{1}$$

where

- $x \in \mathbb{R}^n$ is the state vector of the system under ideal conditions;
- $\tilde{x} \in \mathbb{R}^k$ is the state vector of the imperfect dynamics;
- $u \in \mathbb{R}^m$ is the vector of the exogenous control signals;
- $w \in \mathbb{R}^q$ is the vector of exogenous not controllable signals;
- $p \in \mathbb{R}^g$ is the vector of the system parameters;

and $f : \mathbb{R}^n \times \mathbb{R}^k \times \mathbb{R}^m \times \mathbb{R}^q \times \mathbb{R}^g \times \mathbb{R} \to \mathbb{R}^n$, and $\tilde{f} : \mathbb{R}^n \times \mathbb{R}^k \times \mathbb{R}^m \times \mathbb{R}^q \times \mathbb{R}^g \times \mathbb{R} \to \mathbb{R}^n$ are nonlinear vector fields.

The electromechanical structure described in Sect. 2 can be modeled following the approach presented in [2]. The general framework identifies two interacting dynamics: the spinning of the coil-magnet system and an *hidden* dynamics related to vibrations of the mechanical structure. Therefore, the mathematical model for a round structure with $N = 16$ coils reads as:

$$\begin{cases} \dot{X}_i = Y_i \\ \dot{Y}_i = \frac{1}{J_i}\left(I_i S_i B_i \sin(X_i) - K_i Y_i\right) + \bar{D}_i\left(\tilde{x}_{i+1,1} - \tilde{x}_{i,1}\right) \\ \qquad + \bar{D}_i\left(\tilde{x}_{i-1,1} - \tilde{x}_{i,1}\right) \end{cases} \tag{2}$$

with

$$\begin{cases} \dot{\tilde{x}}_{i,1} = \alpha_i \tilde{x}_{i,2} + u(t) \\ \dot{\tilde{x}}_{i,2} = -\alpha_i \tilde{x}_{i,1} \end{cases} \tag{3}$$

for $i = 1, \ldots, 16$ where X_i and Y_i represent the phase and the angular speed of the i-th coil, respectively, while $\tilde{x}_{i,1}$ and $\tilde{x}_{i,2}$ account for the vibration of the mechanical structure, assumed as sinusoidal. Concerning other parameters, J_i is the angular momentum, and K_i the damping factor. I_i is the current flowing into the coil and is given by

$$I_i = \frac{V_s - Y_i S_i B_i \sin(X_i)}{R(X_i)}$$

with V_s the voltage supplied to the system, S_i the coil area, B_i the magnetic field provided by the i-th magnet and $R(X_i)$ the contact resistance, which, due to the coil construction constraint, is nonlinear according to:

$$R(X_i) = \begin{cases} 0.2\ \Omega & \text{if} \quad X_i < \pi \\ 10\ k\Omega & \text{if} \quad X_i \geq \pi \end{cases}.$$

The friction factor K_i between each coil and its support depends on the angular speed of each coil as

$$K_i = \begin{cases} K_{H,i} & \text{if} \quad Y_i < 2\ \text{Hz} \\ K_{L,i} & \text{if} \quad Y_i \geq 2\ \text{Hz} \end{cases}.$$

Finally, α_i is the natural frequency of the imperfect dynamics associated with the i-th coil ($i = 1, \ldots, 16$), $\bar{D}_i$ are the diffusion coefficients associated with the imperfect dynamics. The signal $u(t)$ is the combined effect of the control action on the system. To take into account the role of uncertainties in the model, the values of the parameters J_i, S_i, B_i, $K_{H,i}$, and $K_{L,i}$ can be chosen from a random Gaussian distributions with mean value μ and variance σ^2. Note that, representing a round structure, toroidal boundary conditions are considered for model (2), i.e., i has to be considered modulo N.

The task that we want to achieve is the complete start-up of the various coils, i.e., the onset of an effective and steady rotation of all coils. The task is nontrivial since the mechanical supports are flexible structures with multiple structure modes. Moreover, the slots where the coils are located are different from each other. All these factors contribute to create adverse conditions to attain the desired working conditions. In particular, depending on the initial conditions and system parameters, when the power is switched on, typically it occurs that some coils start rotating, while others do not. Increasing the power provided to the electromechanical system generally tends to favor the conditions for which all coils starts rotating.

We aim at defining a control strategy which guarantees the desired working conditions also in the presence of limited power supply. In particular, the control system generates a signal which induces an oscillation on the mechanical structure [17], according to the output of the optical sensors monitoring the angular speed of the coils. The output of the sensor array is acquired and processed through a STM32 microcontroller unit Nucleo [18] which implements the on/off switch of the control action. The high-level control signal is fed to the structure if coils are not actually rotating; otherwise, the control is turned off.

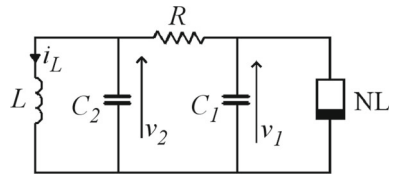

Fig. 7 The Chua's circuit

An extensive analysis of numerical simulations performed on the mathematical model (2) has been carried out and described in [1], when the structure is controlled considering $u(t)$ as a sinusoidal vibration.

The vibrational control signals adopted in the experiments on the electromechanical structure reported in this paper are signals with a broadband spectrum, so that the different modes linked to the imperfect dynamics can be continuously stimulated.

Chaos can be obtained from nonlinear dynamical circuits using simple and cheap off-the-shelf components. Let us consider the paradigmatic example of the Chua's circuit [19,20]. The circuit, whose original scheme is reported in Fig. 7, was introduced by Leon O. Chua and it is known as the first electronic circuit that was intentionally designed to generate chaotic behavior [20].

The dynamical equations regulating the behavior of the circuit are:

$$\begin{aligned} \frac{dv_1}{dt} &= \frac{1}{C_1}[G(v_2 - v_1) - g(v_1)] \\ \frac{dv_2}{dt} &= \frac{1}{C_2}[G(v_1 - v_2) + i_L] \\ \frac{di_L}{dt} &= -\frac{1}{L}v_2, \end{aligned} \tag{4}$$

where $G = \frac{1}{R}$ and $i = g(v_1)$ is the $i - v$ characteristic of a nonlinear resistor. Performing a normalization according to $x = v_1/E_1$, $y = v_2/E_1$, $z = i_L R/E_1$, with $E_1 = 1$ V $\tau = t/RC_2$, $\alpha = C_2/C_1$, and $\beta = C_2R^2/L$, the following rescaled equations can be written:

$$\begin{aligned} \dot{x} &= \kappa\alpha[y - h(x)] \\ \dot{y} &= \kappa[x - y + z] \\ \dot{z} &= \kappa[-\beta y], \end{aligned} \tag{5}$$

where now $h(x)$ represents the only nonlinearity in the circuit and κ is a further parameter accounting for temporal rescaling. The nonlinearity is usually expressed as a piecewise-linear (PWL) function $h(x) = m_1 x +$

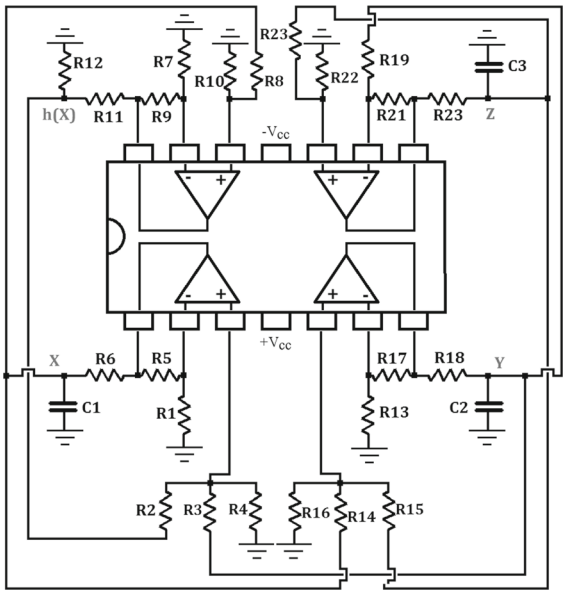

Fig. 8 SC-CNN based circuit implementation of the Chua's equations (5)

$0.5(m_0 - m_1)(|x+1| - |x-1|)$, with m_0 and m_1 system parameters defining the slopes of the PWL. Note that, beyond the nonlinearity often assumed with fixed parameters, only two parameters appear in the Chua's equations, namely α and β.

In order to have a reliable inductor-less circuit, we adopted the SC-CNN based implementation of the Chua's circuit dynamics, as modeled by the dynamical equations (5) with PWL nonlinearity. For the implementation we fix the parameters so that to obtain the double-scroll Chua's attractor: $m_0 = -\frac{1}{7}$, $m_1 = \frac{2}{7}$, $\alpha = 9$, and $\beta = 14.286$.

The circuit is based on off-the-shelf resistors, capacitors and operational amplifiers. The complete scheme is reported in Fig. 8.

The circuit equations associated with the implementation of Chua's circuit are the following:

$$\begin{cases} C_1 R_6 \frac{\mathrm{d}X}{\mathrm{d}\tau} = -X + \frac{R_5}{R_3} Y + \frac{R_5}{R_2} h \\ C_2 R_{18} \frac{\mathrm{d}Y}{\mathrm{d}\tau} = -Y + \frac{R_{17}}{R_{14}} X + \frac{R_{17}}{R_{15}} Z \\ C_3 R_{23} \frac{\mathrm{d}Z}{\mathrm{d}\tau} = -Z + \frac{R_{21}}{R_{20}} Z + \frac{R_{21}}{R_{19}} Y \end{cases}, \tag{6}$$

where

$$h = \frac{R_{12}}{R_{11} + R_{12}} \frac{R_9}{R_8} \left(|X+1| - |X-1|\right), \tag{7}$$

and X, Y, and Z are the voltage across capacitors C_1, C_2, and C_3, respectively.

From the match between Eqs. (5) and (6) it is possible to choose the values of the components, as reported in Table 1. Furthermore, in order to obtain a signal with a spectrum whose main components are in a given range, a temporal rescaling can be introduced suitably choosing $\kappa = \frac{1}{C_2 R_{18}} = \frac{1}{C_3 R_{23}}$.

Furthermore, R_6 is a variable resistor, so that the different dynamical behaviors shown by the Chua's circuit can be retrieved by varying the single bifurcation parameter α. In fact, the parameter is related to the resistor value through the relationship $\alpha = \frac{R_5}{R_3} \frac{R_{18}}{R_6}$.

We used the state variable X, i.e., voltage across capacitor C_1, as control signal. The amplitude is varied according to the needed control law, through the amplifier driving the electromechanical actuators.

4 Experimental and numerical analysis

We now focus on the choice of the location of the two actuators. The driving signal is the same for both actuators to ensure consistency between the two sources in terms of amplitude, frequency and phase. The two actuators can be activated in two different ways on the basis of the direction of the applied forces at the points of stress. It is assumed that the two actuators have an in-phase behavior, when the vectors of the applied forces in the piers have the same direction with respect to their plane. We say that the two actuators have an anti-phase behavior, when the two vectors of the forces applied on the piers are anti-parallel. The different kinds of excitation of the two actuators result in a different mechanical behavior of the structure. In the first case, the whole structure is forced to oscillate along the vertical plane of the active piers, while in the second case, the central ring of the structure is affected by a twisting motion, with respect to the central axis, which leads the whole structure to rotate of an angle proportional to the displacement applied by the actuators. By using a laser sensor Baumer OADM 12U6460/S35A, the displacement Δ of the internal pier of the round structure is measured, when a sinusoidal waveform with constant frequency fixed at 5 Hz is adopted. The data obtained in the two cases discussed above are shown in Fig. 9. Clearly, the anti-phase configuration results in a greater mechanical stress to the structure.

Table 1 SC-CNN based circuit implementation of the Chua's equations (5): component values with $V_{cc} = 9\,V$

Component	Value	Component	Value
R_1	4 kΩ	R_2	13.3 kΩ
R_3	5.6 kΩ	R_4	20 kΩ
R_5	20 kΩ	R_6	380 Ω (potentiometer)
R_7	112 kΩ	R_8	112 kΩ
R_9	1 MΩ	R_{10}	1 MΩ
R_{11}	8.2 kΩ	R_{12}	1 kΩ
R_{13}	51.1 kΩ	R_{14}	100 kΩ
R_{15}	100 kΩ	R_{16}	100 kΩ
R_{17}	100 kΩ	R_{18}	1 kΩ
R_{19}	8.2 kΩ	R_{20}	100 kΩ
R_{21}	100 kΩ	R_{22}	7.8 kΩ
R_{23}	1 kΩ		

Capacitor values are chosen in order to introduce a given temporal scale factor

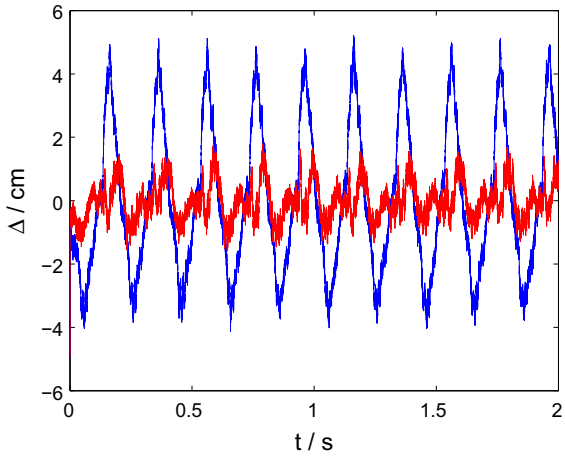

Fig. 9 Displacement Δ of the internal pier of the round structure excited by a pair of anti-phase (blue) and in-phase (red) electromechanical actuators driven by a sinusoidal waveform with frequency 5 Hz. (Colour figure online)

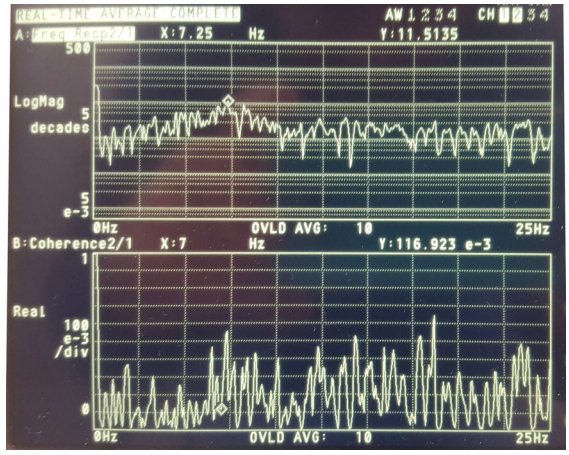

Fig. 10 Experimental evaluation of the frequency response of the round structure with respect to induced vibrations. Displacement is measured by means of the laser sensor located on one supporting pier. Upper panel: frequency response considering as input a sinusoidal waveform used to drive the actuation system and as output the displacement of the rectangular structure measured by the laser sensor. Lower panel: spectral coherence $C_{xy}(f)$

The anti-phase configuration has been then used to identify the frequency response of the round structure by considering as output the displacement of the central pier. A dynamic signal analyzer Agilent 35670A has been used to evaluate the frequency response when a sinusoidal sweep signal is provided to the two actuators and the corresponding spectral coherence $C_{xy}(f)$ [1], in order to estimate the causality relationship between the given input and the considered output. Results are shown in Fig. 10, from which a peak in the frequency response can be retrieved around 7 Hz, a result that leads us to use select for the control a chaotic signal with a spectrum band mainly lying in the same range.

The mathematical model (2) and (3) is able to catch the peculiar properties of the structure, since a complete activation of the rotation of all coils is unlike to occur when no control action is considered and it reveals to be useful to determine the most efficient spectral properties for the control signal. In Fig. 11,

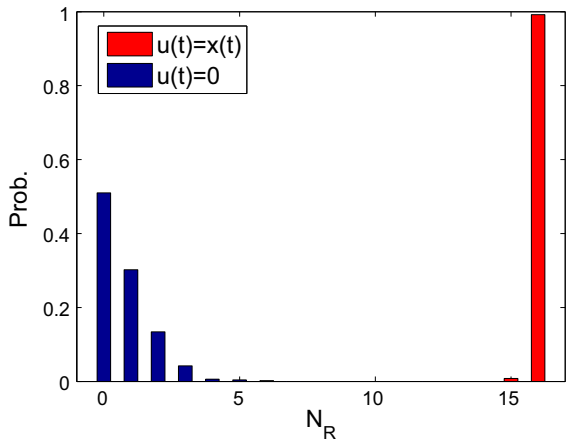

Fig. 11 Numerical simulation of the start-up phase in the model (2): probability of observing N_R rotating coils over 500 realizations. Parameters are randomly chosen for each realization according to a Gaussian distribution with $\langle J_i \rangle = 6 \times 10^{-6}\,\mathrm{g\,m^2}$, $\sigma(J_i) = 10^{-6}$, $\langle S_i \rangle = 3.14 \times 10^{-4}\,\mathrm{m^2}$, $\sigma(S_i) = 10^{-6}$, $\langle \alpha_i \rangle = 10\,\mathrm{rad/s}$, $\sigma(\alpha_i) = 0.5$, $\langle K_{L,i} \rangle = 2 \times 10^{-5}\,\frac{\mathrm{gm^2}}{\mathrm{s}}$, $\sigma(K_{L,i}) = 10^{-6}$, and $V_s = 5\,\mathrm{V}$, $B = 0.008\,\frac{\mathrm{g}}{\mathrm{Am}}$, $\bar{D} = 10$, $K_{H,i} = 10^{-3}\,\frac{\mathrm{gm^2}}{\mathrm{s}}$. Blue histograms: Control action OFF, i.e., $u(t) = 0$ in the simulation; red histograms: control action ON, i.e., $u(t) = x(t)$ with $x(t)$ is the first state variables of the scaled Chua's circuit in the simulation. (Colour figure online)

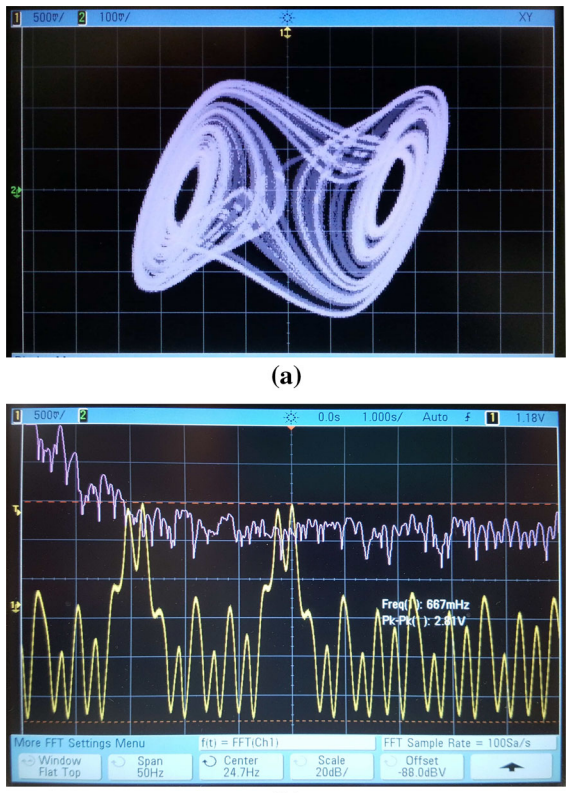

Fig. 12 Oscilloscope traces related to the Chua's circuit: **a** classic double-scroll attractor in the phase-plane X–Y (scales: horizontal 500 mV/div, vertical 100 mV/div), **b** voltage representing the X state variable of the Chua's circuit (yellow trace) and its power spectrum (magenta trace) showing that the main components of the control signal are in the range of 10 Hz. (Colour figure online)

we report the probability of having N_R rotating coils over 500 trials when the term $u(t)$ in Eq. (3), representing the control input to elicit the imperfect dynamics, is set to zero, i.e., no control action is applied, and when $u(t)$ is the $x(t)$ state variable of the Chua's circuit as in Eq. (5) introducing a scaling factor $\kappa = 10$. System parameters have been estimated following [1] and randomly chosen for each realization according to a Gaussian distribution with $\langle J_i \rangle = 6 \times 10^{-6}\,\mathrm{g\,m^2}$, $\sigma(J_i) = 10^{-6}$, $\langle S_i \rangle = 3.14 \times 10^{-4}\,\mathrm{m^2}$, $\sigma(S_i) = 10^{-6}$, $\langle \alpha_i \rangle = 10\,\mathrm{rad/s}$, $\sigma(\alpha_i) = 0.5$, $\langle K_{L,i} \rangle = 2 \times 10^{-5}\,\frac{\mathrm{gm^2}}{\mathrm{s}}$, $\sigma(K_{L,i}) = 10^{-6}$, and $V_s = 5\,\mathrm{V}$, $B = 0.008\mathrm{g/Am}$, $\bar{D} = 10$, $K_{H,i} = 10^{-3}\,\frac{\mathrm{gm^2}}{\mathrm{s}}$.

In Fig. 12, we report the chaotic attractor and the oscilloscope trace of the X variable of the Chua's circuit with its power spectrum, choosing a scaling factor $\kappa = \frac{1}{C_2 R_{18}} = \frac{1}{C_3 R_{23}} = 10$, i.e., fixing $C_1 = C_2 = C_3 = 100\,\mu\mathrm{F}$.

We now want to focus on the performance of the electromechanical structure when power is limited. The system is powered providing a constant voltage V_s to the supporting structure. The current I_s flowing in the supporting trails can be limited by properly setting the power supply, therefore providing a maximum power $P = V_s I_s$ to the electromechanical structure. Without the control action the rigidity of the structure causes that only a fraction of the 16 coils allocated on the supports are actually able to overcome friction and start rotating. Increasing the power supplied the time needed to attain the working condition can be reduced but this represents an inefficient strategy. The vibrations induced by the control strategy allows the coils to start rotating in a shorter time. The effect of the control action can then be evaluated by means of the measure of T_r which is the time needed to reach the working condition, i.e., all coils are actually rotating, when power is limited. In the following, we inspect the performance of the control strategy in terms of T_r with respect to different power conditions and to different control signals.

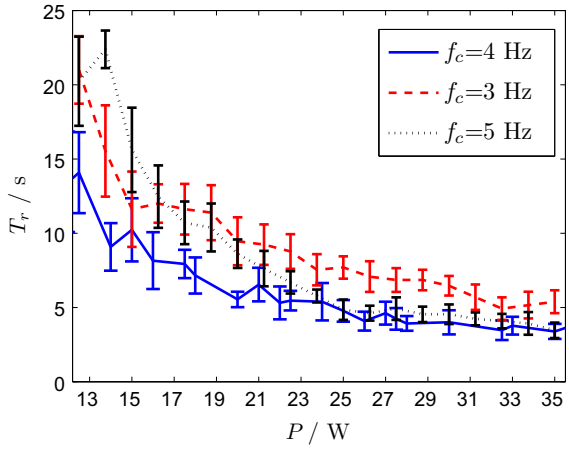

Fig. 13 T_r averaged over 15 trials for different values of the power supply. The three curves are related to three different values of the frequency of the control signal. Error bars account for the standard deviation of each series

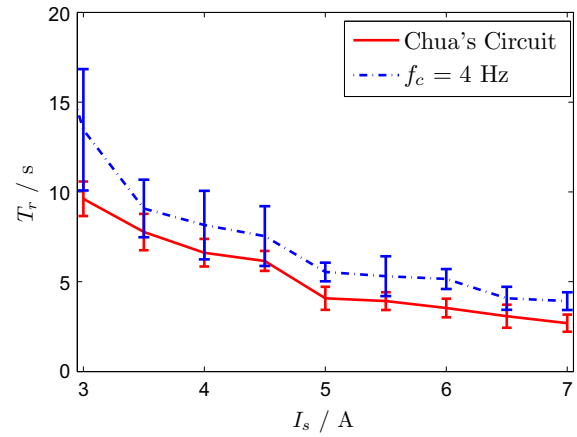

Fig. 14 T_r averaged over 15 trials for different values of the maximum supply current. The two curves are related to the two different strategies to generate the control signal: periodic with frequency $f_c = 4$ Hz, and chaotic as generated by the Chua's circuit in double-scroll. Error bars account for the standard deviation of each series

In order to evaluate the performance of the control action when power supplied to the system is limited, we evaluated the time T_r with respect to the power, maintaining constant the supply voltage to $V_s = 5$ V and controlling the structure with a periodic vibration with amplitude $V_c = 30$ mV and main frequency f_c. The three curves in Fig. 13 report T_r averaged over 15 trials for three different values of the frequency of the control signal.

It should be noted that after T_r, even switching off the control action, all coils keep their spinning motion along their axis, as the sole consequence of the interplay between magnetic and electric fields.

It is interesting to note that the frequency leading to the lowest values of T_r is $f_c = 4$ Hz. This means that the imperfect dynamics is excited at a frequency below the resonance frequency of the system. Moreover, a lower actuation frequency leads to poorer performances as well as stimulating the system at the resonance frequency of the mechanical structure. This latter counterintuitive result is based on the fact that the resonance frequency of the structure and that of the hidden dynamics are different, and stimulating the system at the structure resonance frequency induces strong displacements which prevent the coils rotation.

Let us now introduce the chaotic control signal, using the X state variables of the Chua's circuit in Fig. 12 to drive the actuators. The evaluation of the time T_r and the comparison with the best case of periodic actuation, i.e., $f_c = 4$ Hz are summarized in Fig. 14.

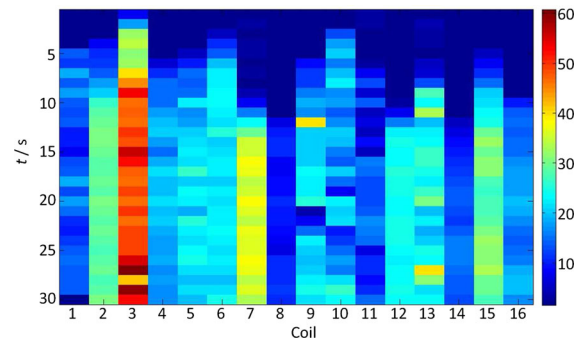

Fig. 15 Angular speed (Hz) of the sixteen coils—excitation with two anti-phase actuators driven by a Chua's circuit X state variables as in Fig. 12

The value of T_r is averaged over 15 trials for $V_s = 5$ V, together with the corresponding error bars, accounting for the standard deviation of the series. As it clearly appears, chaotic vibrations lead to an increase in the control performance with respect to the time needed to complete the start-up phase, thus emphasizing the effectiveness of the approach.

Finally, the pattern of the angular speeds of the coils in the round structure is reported. The measurements cover a period of 30 s and show the variation of the angular speed of each coil averaged on a time window of 1 s. The values are encoded according to the reported colorbar, where dark blue indicates that the coil is not

spinning. Coils are actually spinning in all slots after a time $T_r \approx 10$ s as it can be observed in Fig. 15.

5 Conclusions

In this paper, we investigated the performance of a novel control strategy for imperfect systems. The strategy is based on taking advantage of the unavoidable imperfections, associated with physical realizations, by stimulating the hidden dynamics associated with them. Under these conditions an overall improvement of the system performance can be clearly observed.

We introduced an electromechanical structure whose intrinsic rigidity plays against the correct working conditions. In particular, the structure supporting a number of coils spinning over associated magnets prevents the actual rotation of all of them, since they may not be able to overcome their inertia. The behavior of the system can be improved providing to the structure vibrations with peculiar spectral properties, decreasing the time needed to reach the working condition in which all coils actually rotate. In particular, we focused on the effects of using chaotic vibrational signals to excite the hidden dynamics of the imperfect system.

The interplay between the power supplied to the system and the control signal properties has been deeply discussed, showing the effectiveness of the proposed approach. Even providing low power to the structure, the control action is able to sensibly decrease the time needed to complete the start-up phase. More precisely, the lower is the power, the higher is the advantage introduced by the control action. The control action, therefore, allows for complete start-up of all the coils with the minimum power. We remark that the best control performance occurs when the control action excites the system with broadband signals generated by a chaotic oscillator, thus leading to shorter time needed to complete the start-up phase. This gives clear indication that the effect of the control relies on the excitation of the hidden dynamics rather than that of the mechanical structure and the use of chaos does improve the performance of the control action.

Compliance with ethical standards

Conflict of interest The authors declare that they have no conflict of interest.

References

1. Fortuna, L., Buscarino, A., Frasca, M., Famoso, C.: Control of Imperfect Nonlinear Electromechanical Large Scale Systems: From Dynamics to Hardware Implementation, vol. 91. World Scientific, Singapore (2017)
2. Buscarino, A., Famoso, C., Fortuna, L., Frasca, M.: Passive and active vibrations allow self-organization in large-scale electromechanical systems. Int. J. Bifurc. Chaos **26**(07), 1650123 (2016)
3. Fortuna, L., Buscarino, A., Frasca, M.: Imperfect dynamical systems. Chaos Solitons Fractals **117**, 200 (2018)
4. Braiman, Y., Lindner, J.F., Ditto, W.L.: Taming spatiotemporal chaos with disorder. Nature **378**(6556), 465 (1995)
5. Yim, G.S., Ryu, J.W., Park, Y.J., Rim, S., Lee, S.Y., Kye, W.H., Kim, C.M.: Chaotic behaviors of operational amplifiers. Phys. Rev. E **69**(4), 045201 (2004)
6. Buscarino, A., Fortuna, L., Frasca, M., Muscato, G.: Chaos does help motion control. Int. J. Bifurc. Chaos **17**(10), 3577–3581 (2007)
7. Meerkov, S.M.: Vibrational control. Avtom. Telem. **2**, 34–43 (1973)
8. Liu, H.G., Liu, X.L., Yang, J.H., Sanjuán, M.A., Cheng, G.: Detecting the weak high-frequency character signal by vibrational resonance in the Duffing oscillator. Nonlinear Dyn. **89**(4), 2621–2628 (2017)
9. Jia, P.X., Wu, C.J., Yang, J.H., Sanjuán, M.A., Liu, G.X.: Improving the weak aperiodic signal by three kinds of vibrational resonance. Nonlinear Dyn. **91**(4), 2699–2713 (2018)
10. Hunnekens, B.G.B., Fey, R.H.B., Shukla, A., Nijmeijer, H.: Vibrational self-alignment of a rigid object exploiting friction. Nonlinear Dyn. **65**(1–2), 109–129 (2011)
11. Yildirim, H., Nwokah, O.D.I.: The Mechanical Systems Design Handbook: Modeling, Measurement, and Control. CRC Press, Boca Raton (2016)
12. Moskowitz, L.R.: Permanent magnet design and applications handbook. Krieger Publishing (1995)
13. Webster, J.G., Eren, H. (eds.): Measurement, Instrumentation, and Sensors Handbook: Electromagnetic, Optical, Radiation, Chemical, and Biomedical Measurement. CRC Press, Boca Raton (2014)
14. Busch-Vishniac, I.J.: Electromechanical Sensors and Actuators. Springer, Berlin (2012)
15. Skvarenina, T.L. (ed.): The Power Electronics Handbook. CRC Press, Boca Raton (2001)
16. Mohan, N., Undeland, T.M., Robbins, W.P.: Power Electronics. Wiley, New York (1988)
17. Gawronski, W.: Balanced Control of Flexible Structures. Springer, Berlin (2006)
18. ST Microelectronics (2014). http://www.st.com/web/en/catalog/mmc/FM141/SC1169/SS1576?sc=stm32f3
19. Madan, R.N. (ed.): Chua's Circuit: A Paradigm for Chaos. World Scientific, Singapore (1993)
20. Fortuna, L., Frasca, M., Xibilia, M.G.: Chua's Circuit Implementations: Yesterday. Today and Tomorrow. World Scientific, Singapore (2009)